Mesoscale structure of neuston assemblages across the southern Indian Ocean subtropical gyre

Mark J. Gibbons [a,*], Yasmeen Parker [a], Riaan B. Cedras [a], Delphine Thibault [b]

[a] *Department of Biodiversity and Conservation Biology, University of the Western Cape, 7535, South Africa*
[b] *Aix Marseille Univ, Université de Toulon, CNRS, IRD, MIO, Marseille, France*

ARTICLE INFO

ABSTRACT

Despite concern around plastic pollution in subtropical gyres, our understanding of the biological component of the neustonic layer (upper 20 cm of the ocean) in these areas is poor. Here we investigate the neuston (excluding copepods) assemblages across the Southern Indian Subtropical Gyre using triplicate samples collected by manta-trawls from 28 stations along a transect at latitude 20 S during June/July 2015. The vertical structure of the water column at each station was assessed using a CTD. With the exception of siphonophores, all non-copepod neuston were identified to morphospecies. Assemblages were dominated by ostracods, mysids, larval chaetognaths and siphonophores. The majority of collected specimens comprised facultative neuston, which were more common at night than during the day. Neuston assemblages from the east were quite distinct from the balance of samples, and their distribution reflected that of the warm, low salinity water associated with the Indonesian Throughflow. Two anticyclonic eddies had been documented at the time of the survey between 70 and 85° E, and this area was associated with a distinct neuston assemblage of generally low abundance. The key environmental factors that were linked to assemblage structure were associated with longitude – salinity, fluorescence and temperature at 200 m, emphasising the interaction between Indonesian Throughflow Water and the South Equatorial Current, eddy-related process and settlement of meroplankton. The study highlights the value of using morphospecies in studies of plankton assemblages.

1. Introduction

Global winds, driven by latitudinal pressure gradients, transfer energy to surface waters to create shallow currents which, under the influence of the Coriolis force and through interactions with continental land masses, form anticyclonic gyres in the central ocean basins north and south of the equator (Mann and Lazier, 2006). These subtropical gyres transport large quantities of heat away from the equator in meandering western boundary currents that in turn may generate cold- and warm-core rings/eddies (Mann and Lazier, 2006). Oceanic waters of subtropical gyres are permanently stratified, nutrient depleted with a low level of productivity (Brix et al., 2004; Follows et al., 2002; Williams and Follows, 2011), but it is known that production can be increased by the presence of mesoscale eddies through eddy pumping (McGillicuddy and Robinson, 1997) and by Ekman transport from peripheral gyres (Mann and Lazier, 2006). Indeed, Dufois et al. (2016) have recently suggested that anticyclonic subtropical gyres may contribute 50% towards the global ocean organic carbon pump, largely because

eddy-induced mixing in surface layers during winter provides high levels of nutrients that then fuel elevated primary production.

Zooplankton assemblages within the epipelagic layer (upper 200 m) of subtropical gyres are thought to be remarkably stable across a variety of spatial and temporal scales (e.g. McGowan and Walker, 1985), and this has been attributed to the very strong nature of biological interactions. Depth, on the other hand, is considered to have a profound impact on structuring habitats and associated communities as shown in their global study of low latitude zooplankton assemblages by de Puelles et al. (2019). That said, changes in zooplankton assemblage composition and structure are apparent when moving away from continental landmasses (Piontkovski et al., 2003). González et al. (2019) noted a transition from eutrophic to ultra-oligotrophic assemblages moving westward along latitude ~28 S from South America to the centre of the South Pacific Subtropical Gyre. At the mesoscale, zooplankton abundance and diversity in the centre of subtropical gyres tends to be lower than observed at the edges (Piontkovski et al., 2003; González et al., 2019), which possibly reflects the generally lower productivity observed

there.

Neuston is a special type of plankton that inhabits the sea-air interface (Naumann, 1917; Zaitsev, 1971), and it can be categorised into three major ecological groups; euneuston (epi- and hypo-neuston), facultative neuston and pseudoneuston (Hempel and Weikert, 1972; Helm, 2021a). The euneuston comprises organisms permanently inhabiting the neustonic realm, day and night, and it is most abundant in the direct vicinity of the ocean surface (e.g. *Halobates* spp., *Velella velella*, *Glaucus atlanticus*). Facultative neuston inhabit the surface of the ocean temporarily, usually during part of diel vertical migration cycles (e.g. some pontellid copepods), whilst pseudoneuston is most common at depth but may be found at the surface. The composition of neuston assemblages can be diverse (Hempel and Weikert, 1972; Weikert, 1970; Holdway and Maddock. 1983a; Mojib et al., 2017), and a number of taxa have larvae that favour this ecotone for at least part of their lives (Whitney et al., 2021). Most euneustonic taxa have evolved morphological and/or ecophysiological adaptations to this environment, which makes them different from more typical zooplankton (e.g. Herring, 1967; Ianora et al., 1992; Andersen and Cheng, 2004; Rahlff et al., 2018). Consequently, the factors that drive assemblage structure tend to be slightly different from those of more typical zooplankton (Collard et al., 2015), though pronounced diel changes are noted owing to the migration of facultative forms (Hempel and Weikert, 1972).

While our understanding of the zooplankton assemblages associated with subtropical gyres is thin by comparison with those of more temperate or coastal waters, our knowledge of neuston assemblages there is far worse. And this despite the fact that subtropical gyres are widely considered as concentrators of microplastics (Goldstein et al., 2012; Eriksen et al., 2013; Brach et al., 2018), especially at the air-sea interphase (Thiel and Gutow, 2004), and that these "garbage patches" are receiving increasing international attention (e.g. Lebreton et al., 2018).

The Indian Ocean is regarded as less well studied than either the Atlantic or the Pacific oceans (Hood et al., 2016), though recent research suggests that the subtropical gyre in the southern basin too is associated with elevated chlorophyll during winter (Toresen et al., 2015; Dufois et al., 2017). Unfortunately, matching information on zooplankton is scant. The aim of this study is two-fold. Firstly, it is to describe the non-copepod neuston across the Southern Indian Ocean Gyre and secondly it is to examine changes in assemblage structure across the region, and to link such changes (where possible) to variations in the oceanographic environment observed by Toresen et al. (2015) and Dufois et al. (2017). It is hypothesised, following González et al. (2019), that neuston assemblages in the vicinity of the eddies at the centre of the gyre will be distinct from the balance. Following Hoeksema (2007) it is also anticipated that assemblages closer to landmasses will comprise greater numbers of meroplanktonic taxa and that there would be a higher abundance of neuston during the night than during the day (Holdway and Maddock, 1983a).

2. Materials and methods

2.1. Field sampling

A total of 28 stations were sampled at regular intervals (100 nautical miles, 150 nautical miles) along a transect line extending from Jakarta, Indonesia to Port Louis, Mauritius, between 26 June - 16 July 2015 onboard the RV *Dr Fridtjof Nansen* during the EAF-Nansen programme GCP/INT/003/NOR and the Second Indian Ocean Expedition (IIOE2) (Fig. 1) (Toresen et al., 2015). At each station, vertical profiles of temperature, salinity, oxygen, and fluorescence were conducted using a Seabird 911+ CTD fitted with a Turner Design fluorometer from the surface to 200 m.

Although it is customary to take a single neuston sample at any station (e.g. Jeong et al., 2014; Albuquerque et al., 2021), here we collected three neuston samples (total = 84) at each. Individual stations were not occupied for a full day-night cycle, but were sampled sequentially along the transect line, so there is no corresponding set of day and night samples for any station. Although statistically-speaking the triplicate samples are pseudo-replicates for each station, patchiness in plankton assemblages is marked even at small spatial scales (e.g. de Wolf, 1989). Rather than pool the triplicates (average or sum), we have elected to retain the full information content of each sample and to treat each as a "replicate". These were collected using a rectangular manta trawl (mouth frame 15 cm high by 31 cm wide) balanced by two wings and fitted with a net (mesh size 335 μm) and a 100 mL cod end. The net was deployed on the forward starboard side of the vessel only in relatively calm weather (wave height <2m), for 15 min at a speed of 2-3 knots (Toresen et al., 2015; Bernal et al., 2020). On retrieval, the net was washed down from the outside and the contents of the cod-end passed through a 180 μm mesh sieve. Microplastics were removed (Bernal et al., 2020) and the neuston was fixed/preserved in either 96% ethanol or 4% buffered seawater formalin for later processing in the laboratory (Toresen et al., 2015). As no flowmeter was used, the abundance of neuston taxa can only be given per haul.

2.2. Laboratory methods

Prior to microscopic examination, those samples in formalin were drained through a 180 μm sieve and material was suspended in
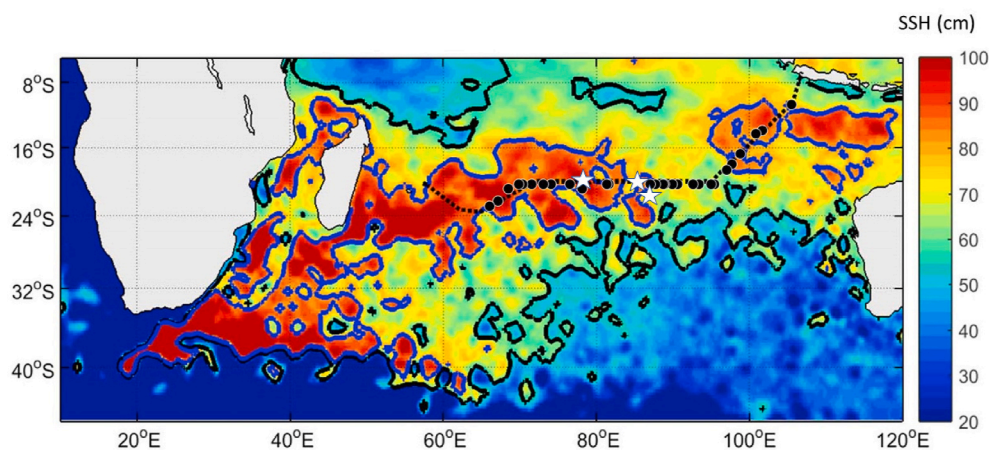

Fig. 1. Mean Sea Surface height (SSH, cm) during the cruise, derived from satellite data on July 09, 2015. The main black and blue contours highlight the outer edge and the central part of the South Indian Ocean subtropical gyre, respectively. The dotted line represents the cruise track, the black circles indicate the position of neuston samples and the white stars denote the positions of the three eddies observed by Dufois et al. (2017). Figure adapted from Bernal et al. (2020).

freshwater: samples in ethanol were examined without rinsing. All samples were examined (and specimens counted) under a dissecting microscope at various magnifications without sub-sampling and, with the exception of siphonophores, were identified to morphospecies. Photographs of most of the morphospecies identified are provided in Supplementary Material A: images of obvious taxa (e.g. juvenile chaetognaths) are not provided. In the case of siphonophores, specimens were identified to species level, and images of these are not provided. Calycophorae were identified using, and counted from, the anterior nectophores of the polygastric stage, except for Hippopodidae which were, as Physonectae, identified from their nectophores and their presence/absence noted. Copepods were not included in this study, but were set aside for further analysis.

It is customary in ecological studies to identify sampled specimens to the lowest taxonomic level using morphological characters. Ideally, this is to the level of species, as defined by the Darwinian concept of a species (Darwin, 1859; Pos et al., 2014). In practice, however, this becomes difficult when samples are diverse and contain a large number of very different taxonomic groups, because the expertise needed to identify all sample members to species level is not available. In such circumstances, there is a tendency to focus on a taxonomically distinct and well-known taxon – a taxocene (Morin, 2011). It is then generally assumed that observations from the well-known can be extrapolated to the unknown (Morin, 2011). Although this assumption can sometimes be supported (e.g. Pakhomov et al., 2000 cf Kuyper et al., 2020), depending on the question being asked, there are instances when it cannot (Morin, 2011).

When attempts are made to identify everything to the lowest taxonomic level, individuals that cannot be distinguished are often recorded as "indets", and the number of indets will increase as the dataset increases (Pos et al., 2014). Deciding whether to incorporate or ignore these individuals in subsequence analyses can become tricky as they are associated with their own errors. Consequently, there is little agreement among ecologists on how "indets" should be treated and to what degree they may compromise the results (Pos et al., 2014).

An attempt is made here to be as inclusive as possible, and to use all the material in the samples. However, given our lack of taxonomic expertise, it has been decided to use morphospecies. As samples were processed, specimens with a readily identifiable morphology were photographed, put aside as vouchers, and provided with unique labels, so that it was possible to validate and cross-reference subsequent identifications (Supplementary Material A). "Indets" are consequently accorded taxon-level recognition because, with the exception of siphonophores, all specimens are "indets". It is acknowledged that in some cases, one morphospecies may comprise more than one real species and it is understood that in other cases more than one morphospecies could be assigned to a single species – especially in the case of larval decapods and fish larvae where different developmental stages may look quite different from one another. However, the error is assumed to be consistent as only one person was involved in morphospecies designation and sample analysis.

Additional information was also provided for each taxon regarding its main feeding behaviour (herbivorous, omnivorous or carnivorous) as well as information on their life cycle (i.e. holoplanktonic or meroplanktonic).

2.3. Data analyses

Temperature, salinity, and chlorophyll/fluorescence were recorded in order to see if there were any cohesive changes in the environment across the transect. Vertical profiles were constructed using the computer package Ocean Data View version 5.2.0. Even though neuston occur within the upper 20 cm of the water column (Naumann, 1917), the vertical profiles were constructed to a depth of 200 m in order to describe and assess the environment of migratory species. It should be remembered that most of the samples were collected in an equatorial region where productivity is typically low at the surface and biomass generally peaks at some depth (Stramma and Lutjeharms, 1997).

In order to examine multivariate patterns in the assemblages sampled across the Southern Indian Ocean Gyre, data were analysed using various software at the level of morphospecies (Supplementary Material A). Patterns in community structure were assessed, *a priori*, by binning stations into a) 5° Longitudinal Class[es] and b) Time of Day (day, dusk, night). The rationale behind this was twofold. Firstly, our aim was primarily to determine if there were east-west changes in the structure of neuston assemblages across the subtropical gyre, but owing to the patchy nature of samples, it was necessary to bin them into 5-degree bins. And secondly, it is understood that the composition and structure of neuston assemblages varies with time of day (Zaitsev, 1971). Time of day was assessed from the sample log with reference to The NOAA Solar Calculator (https://www.esrl.noaa.gov/gmd/grad/solcalc/) remembering that the ships log was set as UTC (GMT): dawn and dusk were designated as the times of sunrise and sunset ± 1 h, respectively.

The biological data were first root-root transformed and a Bray-Curtis similarity matrix was computed between samples. In order to determine if there was an effect of both longitude and time of day on overall assemblage structure, data were analysed using a PERMANOVA (permutational MANOVA), with the factors Longitude Class and Time of Day set as fixed and random, respectively. Otherwise default settings were used: Type III sum of squares, permutation of residuals under a reduced model and fixed effects sum to zero for mixed terms (Anderson et al., 2008). These analyses were performed using PRIMER v7 + PERMANOVA software (Clarke and Gorley, 2015). Facultative and euneuston were treated separately, in the first instance.

Given the significant effect of Time of Day on assemblage structure (see below), data were analysed separately for Day and Night samples; Dusk and Dawn samples were omitted from the analyses, being too few. Separate similarity matrices were constructed for Day and Night samples, and the significance of a spatial pattern was tested using a one-way ANOSIM. A matrix of pairwise R values between Longitude Class was computed, which was visualised using cluster analysis with group-average sorting. These analyses were conducted using PRIMER v7 software (Clarke and Gorley, 2015).

To test for differences in the average abundance of neuston across samples by Time of Day (Day vs Night) and longitude, a two-way full factorial ANOVA was performed on $\log_{10}$ transformed data, excluding night-time samples from Longitude Class 85 (80–85° E), owing to the absence of matching daytime data. Similar tests were computed for the other univariate measures that summarise assemblages, namely species richness (root transformation) and diversity (H′). Species diversity per sample was computed using the Shannon Index (H'), following Krebs (1999).

The morphospecies responsible for 70% of the similarity (identity) of samples by Time of Day and Longitude Class were determined using a Similarity Percentage analysis (SIMPER). Data were pooled by Longitude Class and Time of Day, respectively, in these analyses since there were too few data to generate robust patterns if they had been partitioned. These analyses were conducted using PRIMER v7 software (Clarke and Gorley, 2015).

A Distance Based Linear Model (DistLM) was computed to determine the environmental variables driving assemblage structure by day and night separately. The predictors used included sea surface temperature and salinity, the temperature and salinity at 200 m, the depth of the upper mixed layer and of the fluorescence maximum as well as integrated fluorescence, and the fluorescence value at the fluorescence maximum. Marginal and sequential tests were performed by stepwise selection and the significance of model outputs was assessed using adjusted R^2. Owing to some fairly large gaps in the environmental data (especially for fluorescence), analyses were confined only to those samples with matching environmental data.

Information on the abundance of microplastics (numbers per manta

trawl) have been published by Bernal et al. (2020). Here we simply investigate the correlation between microplastic abundance and the abundance of both facultative neuston and euneuston (separately) using Pearson's correlation coefficient (*R*), following $\log_{10}$ transformation.

3. Results

3.1. Hydrography

Hydrographic data have already been presented elsewhere (Dufois et al., 2017). In summary, these authors noted the presence of three eddies: one cyclonic eddy near 89°E the smallest of the three and with a lifespan of 70 days and two anticyclonic eddies at approximately 78.5°E and 87°E. with a lifespan between 117 and 132 days (Dufois et al., 2017).

Surface waters were generally warmer than 23 °C across the transect (Fig. 2), being warmest (>26 °C) and fresher (<34.75) off Christmas Island to the east as a result of the Indonesian Throughflow (e.g. Feng et al., 2018). This latter feature plays an important role in the transport of salt and heat from the Pacific Ocean (Feng et al., 2018) and can be
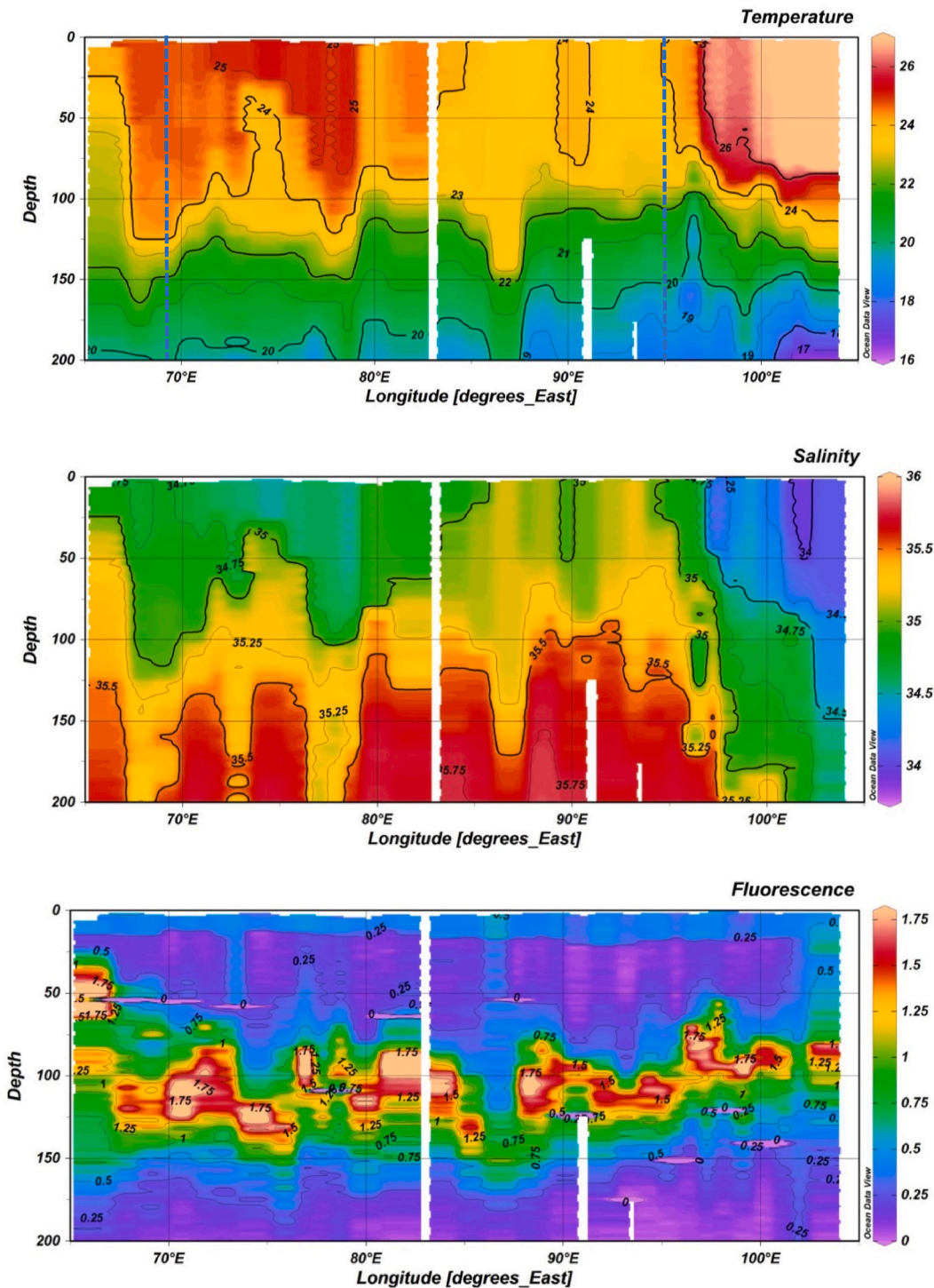

Fig. 2. Vertical profiles (depth in m) of temperature, °C (a), salinity (b) and fluorescence (c) observed across the Southern Indian Subtropical Gyre during June/ July 2015.

detected here as far west as ~ 100°E, at the surface (Fig. 2). One of the two anticyclonic eddies noted by Dufois et al. (2017), centred on ~ 79°E, can be clearly seen in the vertical profiles of both temperature and salinity (Fig. 2), while that at ~87° E cannot. Although the ocean temperature remained above 23 °C down to 100 m, an upward doming of cooler isotherms is noted east of ~90°E, perhaps reflecting the cyclonic gyre noted in that region (Dufois et al., 2017). The DCM (Deep chlorophyll maximum) across the transect was centred at ~ 120 m, except in the extreme west where it was much shallower at ~45 m (Fig. 2). Dufois et al. (2017) noted that the vertical position of the chlorophyll maximum closely tracked the mixed-layer depth.

3.2. Neuston

3.2.1. Assemblage composition

Overall, 133 morphospecies belonging to 7 phyla were collected over the whole transect (Supplementary Material B). Arthropoda, Cnidaria and Gastropoda displayed the highest number of morphotypes with 52, 32 and 23 respectively while Fish and Thaliacea were composed of 12

and 7 morphotypes respectively. Calycophorae, Hyperiidae and Pteropoda alone totalised 52 morphospecies (Table 1) with 18, 18, and 16 species/morphospecies, respectively. Twenty-one morphotypes were present at 50% or more stations while twelve occurred at 10 or less stations. Calycophorae occurred at all stations, and decapod larvae and fish were noted at 96.4% and 92.9% of the stations, respectively. Euneuston was represented by eight species/morphospecies (Anthoathecata- *Porpita porpita* and *Vellela velella*; Cystonectae – *Physalia physalis*, three morphospecies of *Halobates* spp., as well as the gastropods *Glaucus* sp. and *Janthina* sp.).

Ostracods, mysids, juvenile chaetognaths and calycophoran siphonophores (Table 1) represented ~70% of the neuston abundance with average abundance (± se) over the whole transect of 81.81±36.01, 61.23 ± 13.15, 52.07 ±10.20 and 24.81 ± 3.00 ind haul^{-1} respectively.

3.2.2. Effects of longitude and time of day on assemblage structure

Although Longitude Class did not appear to impact facultative neuston assemblages across the transect (Table 2), the results from the PERMANOVA routine indicated that both *a priori* factors influenced the

Table 1
The number of morphospecies (N), frequency of occurrence (%F) across sampling stations and average abundance per haul of the major taxa recovered in neuston samples across the Southern Indian Ocean Gyre during winter 2015. Average abundance expressed across all stations (ALL), or across indicated Longitude Classes. Also shown is the approximate trophic group (O, omnivore; C, carnivore; H, herbivore) and holoplanktonic/meroplanktonic characteristics of the taxa. Presence of Physonectae (+), absence of taxa (−), as well as euneuston (*) taxa are indicated.

Taxon 1	Taxon 2		N	Diet	Holo/Mero	% F	Mean Abundance±stdev per Longitude Classes (number stations)				
							ALL	65-70°E (3)	70-85°E (9)	85-95°E (10)	95-105°E (6)
Cnidaria	Hydrozoa	Anthoathecata*	3	C	Holo/Mero	92.9	10.04± 1.59	20.56± 4.56	9.04± 1.90	12.27± 3.59	2.56± 0.99
		Tracymedusae	1	C	Holo	3.6	0.01± 0.01				0.06± 0.06
	Siphonophora	Calycophorae	18	C	Holo	100.0	24.81± 3.00	30.22± 13.58	23.67± 3.18	29.43± 6.63	16.11± 2.50
		Cystonectae*	1	C	Holo	32.1	0.19± 0.06	0.22± 0.15	0.04± 0.04	0.07± 0.05	0.61± 0.23
		Physonectae	3	C	Holo	10.7	+	–	+	–	+
	Scyphozoa	Scyphozoa	5	C	Holo/Mero	14.3	0.2± 0.11	–	–	0.07± 0.05	0.83± 0.50
	Zoantharia	Larvae	1	O	Mero	50.0	0.29± 0.07	1.11± 0.48	0.19± 0.08	0.1± 0.06	0.33± 0.11
Tunicata	Thaliacea	Doliolida	1	H	Holo	60.7	0.87± 0.23	1.11± 0.45	0.19± 0.09	0.97± 0.49	1.61± 0.66
		Pyrosomatida	1	H	Holo	7.1	0.04± 0.02	–	0.11± 0.06	–	–
		Salpida	5	H	Holo	96.4	2.7± 0.46	2.22± 0.49	2.44± 0.69	2.83± 1.06	3.11± 0.74
Craniata	Fish	Fish	12	C	Mero	92.9	1.98± 0.37	0.44± 0.24	1.37± 0.31	1.33± 0.26	4.72± 1.47
Arthropoda	Ostracoda	Ostracoda	4	O	Holo	78.6	81.81± 36.01	4.11± 3.04	3.56± 1.16	18.77± 5.21	343.11± 156.01
	Decapoda	Brachyura	1	O	Mero	50.0	2.39± 0.82	1.89± 1.11	0.22± 0.15	3.2± 2.00	4.56± 1.71
		Sergestidae	1	C	Holo	5.9	0.17± 0.09	0.22± 0.22	0.44± 0.26	–	–
		Larvae	6	O	Mero	96.4	2.56± 0.47	4.67± 1.91	1.15± 0.44	3.03± 0.68	2.83± 1.45
		Lucifer	1	C	Holo	71.4	13.02± 4.88	59.22± 30.37	0.44± 0.22	5.47± 2.20	21.39± 15.04
	Euphausiacea	Adult	2	O	Holo	3.6	0.06± 0.06	–	–	0.17± 0.17	–
		Larvae	1	H	Holo	67.9	6.77± 2.32	8.89± 5.33	8.04± 3.28	2.07± 0.72	11.67± 9.25
	Amphipoda	Gammaridea	6	O	Holo	78.6	16.56± 3.03	16.33± 9.00	7.26± 1.74	14.97± 3.48	33.28± 11.16
		Hyperiidea	18	C	Holo	92.9	11.69± 2.06	8.33± 2.49	11.33± 3.83	10.03± 3.90	16.67± 4.00
	Isopoda	Isopoda	1	H	Mero	28.6	0.15± 0.05	–	0.07± 0.05	0.37± 0.11	–
	Mysida	Mysida	1	O	Holo	85.7	61.23± 13.15	129.56± 74.16	20.19± 7.54	36.03± 12.87	130.61± 37.59
	Insecta	Water strider*	3	C	Holo	82.1	4.57± 1.01	4.33± 2.09	2.7± 0.77	0.27± 0.11	14.67± 3.54
	Stomatopoda	Stomatopoda	7	C	Mero	71.4	2.32± 0.54	1.78± 0.92	0.33± 0.17	3.53± 1.16	3.56± 1.37
	Cirripedia	Cypris larvae	1	H	Mero	64.3	1.07± 0.27	1.00± 0.33	0.67± 0.18	1.47± 0.67	1.06± 0.53
Chaetognatha	Chaetognatha	Chaetognatha	1	C	Holo	92.9	52.07± 10.20	121.44± 58.89	4.33± 2.57	63.53± 18.44	69.89± 14.07
Mollusca	Gastropoda	*Janthina**	1	C	Holo	71.4	1.5± 0.26	2.78± 0.89	1.59± 0.41	1.7± 0.54	0.39± 0.16
		Larvae	1	H	Mero	3.6	0.01± 0.01	–	0.04± 0.04	–	–
		Heteropoda	2	C	Holo	53.6	0.51± 0.13	0.56± 0.29	0.41± 0.17	0.33± 0.13	0.94± 0.50
		Nudibranchia*	1	C	Holo	3.6	0.04± 0.04	–	0.11± 0.11	–	–
		Pteropoda	16	H	Holo	92.9	8.8± 1.83	4.44± 0.78	10.11± 3.51	3.67± 0.73	17.56± 6.23
	Cephalopoda	*Spirula*	1	C	Holo	3.6	0.01± 0.01	–	–	0.03± 0.03	–
		Larvae	2	C	Mero	14.3	0.05± 0.02	–	0.04± 0.04	0.1± 0.06	–
Annelida	Polychaeta	Alciopid	3	C	Holo	21.4	0.1± 0.04	0.22± 0.15	0.11± 0.08	0.03± 0.03	0.11± 0.08
		Larvae	1	H	Holo/Mero	7.1	0.24± 0.15	–	0.41± 0.33	–	0.5± 0.5
		Tomopteridae	1	C	Holo	3.6	0.01± 0.01	–	–	–	0.06± 0.06
	Sipuncula	larvae	1	O	Mero	3.6	0.01± 0.01	–	0.04± 0.04	–	–

Table 2
PERMANOVA results to examine the effects of Time of Day and Longitude on the structure of neuston assemblages across the Southern Indian Ocean Subtropical Gyre in winter 2015. A, all neuston; B, facultative neuston; C, euneuston.

A: All neuston							
Source	DF	SS	MS	Pseudo-*F*	*p*(perm)	No Unique Permutations	P(MC)	Estimate of components of variation
Longitude Class	7	36769	5252.6	1.5009	0.038	997	0.022	190.94
Time of Day	3	22327	7442.3	5.1771	0.001	999	0.001	405
Longitude Class x Time of Day	9	31899	3544.4	2.4656	0.001	997	0.001	513.71
Residual	64	92002	1437.5					1437.5
B: Facultative neuston								
Longitude Class	7	34940	4991.5	1.3414	0.111	998	0.065	7
Time of Day	3	23760	7920	5.1703	0.001	998	0.001	3
Longitude Class x Time of Day	9	33917	3768.6	2.4602	0.001	996	0.001	9
Residual	64	98037	1531.8					64
B: Euneuston								
Longitude Class	7	45215	6459.3	2.616	0.028	999	0.017	7
Time of Day	3	11074	3691.5	3.559	0.001	998	0.001	3
Longitude Class x Time of Day	9	22395	2488.3	2.399	0.002	998	0.002	9
Residual	61	63270	1037.2					61

structure of neuston assemblages in the region, despite the high residual sums of squares (Table 2). As a consequence, data have been treated separately by Time of Day in all subsequent analyses. Similar conclusions are reached from two-way, full factorial ANOVA on the whole assemblage, which indicates that the total abundance of the neuston in the samples was significantly impacted by Time of Day (Fig. 3), Longitude Class and the interaction between both factors (Table 3). Abundance was higher during the night than the day and tended to be higher at the extremes of the transect and lowest around 80° E (Table 4). Effectively, similar temporal results were observed in terms of sample diversity, either measured as richness or diversity (Table 4), though there was no clear spatial pattern.

The average abundance (±se) of those morphospecies that were responsible for 70% of the dissimilarity (SIMPER analysis) between Day and Night samples (across Longitude Class) are shown in Fig. 4. The majority of taxa increased in abundance at night, including some members of the euneuston (*Velella vellela*, *Halobates* spp.); only *Lucifer* and juvenile chaetognaths were more common during the day than at night.

The results of the ANOSIM indicate that there was a significant difference in the structure of the overall neuston assemblages across the transect, by Day (global $R = 0.432$, $p < 0.005$), Night (global $R = 0.439$, $p < 0.005$) and overall (global $R = 0.25$, $p < 0.005$). Similar results were observed when the data for facultative and euneuston were examined separately, being (respectively): Day - $R = 0.37$, $p < 0.005$; $R = 0.19$, $p < 0.05$: Night - $R = 0.38$, $p < 0.005$; $R = 0.43$, $p < 0.005$: overall - $R = 0.20$, $p < 0.005$; $R = 0.23$, $p < 0.005$. Interestingly, there was no significant similarity between the matrices of pairwise R values ($Rho = -0.04$, $p =$

0.57) generated for facultative and euneuston, implying that the longitudinal structure of the two assemblages is distinct.

The cluster analyses generated from the matrices of pairwise R values are shown in Fig. 5 and in Supplementary Material C, and they reveal some interesting patterns. In the case of the samples collected during the day (Fig. 5a), those between 100 and 105°E were very different from the balance, as too were those between 75 and 80°E: no samples were collected between 80 and 85°E (Fig. 5a). The same analysis computed on the night-time data indicate that assemblages between 80 and 85°E were distinct from the balance (Fig. 4b), and that those at the extremes of the transect (between 65 and 75°E; 95–105°E) were more similar to each other than to those immediately surrounding 85°E (Fig. 5b). Examination of the cluster analysis for all data (Fig. 5c) indicates that samples from between 95 and 105°E were more similar to each other than to the rest of the samples; and that those between 70 and 85° E were distinct from the balance. There is a clear pattern in the abundance of meroplankton, which were least common in the centre of the transect than at its periphery (Fig. 6).

The patterns of similarity amongst Longitude Class for the facultative neuston (Supplementary Material Ca) indicate that stations between 70 and 85° E were distinct from the balance, and that those to the east of the transect were also more similar to each other. In the case of the euneuston (Supplementary Material Cb), the most distinct stations were those in the east (95–105° E), with the balance of stations separating out to the west and east of 80° E.

The average abundance (±se) of those morphospecies that were responsible for 70% of the dissimilarity (SIMPER analysis) between the three longitudinal clusters (across Time of Day) identified in Fig. 5c are shown in Table 5. Although all taxa were found across the transect, some did display a pattern of spatial distribution. From this, assemblages between 95 and 105°E were characterised by high numbers of mysids and Ostracod 3, Amphipod 1 = 2 and *Halobates* B, whilst assemblages between 70 and 85°E supported generally low numbers of all but mysids.

Assemblages in the east were dominated by omnivorous taxa (75% - Table 1), and carnivorous morphospecies represented only 21% of taxa. By contrast, carnivorous morphospecies dominated assemblages between 70 and 85°E (50%) and between 65 and 70°E, 85–95°E (56%): omnivores accounted for 30% and 40% of morphospecies in these two areas, respectively (Table 1).

3.2.3. Environmental divers of neuston assemblage structure

The results of the DistLM are shown in Tables 6 and 7, for Day and Night samples, respectively. The results of the marginal tests indicate that two of the predictors associated with fluorescence were significantly related to the longitudinal structure of the day-time assemblages (Table 6a), and that only the fluorescence value at the fluorescence
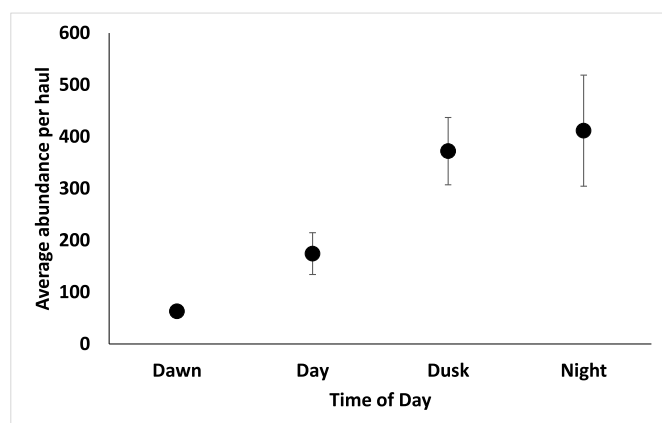

Fig. 3. Diel changes in the mean abundance (±se) of neuston assemblages across the Southern Indian Subtropical Gyre during June/July 2015.

Table 3
Results of two-way, full factorial ANOVA testing the effect of Longitude Class, Time of Day and the interaction between Longitude Class and Time of Day on neuston abundance, sample diversity and sample species richness.

Measure	Abundance		Species Richness		H′	
Statistic/Significance	F	p	F	P	F	P
Intersect	2500.652	<0.0001	2239.530	<0.0001	1047.593	<0.0001
Longitude	10.866	<0.0001	2.701	0.023	2.750	0.021
Time of Day	23.107	<0.0001	39.490	<0.0001	2.613	0.112
Longitude x Time of Day	5.563	<0.0001	2.341	0.045	1.255	0.294

Table 4
Diel changes in the average (±se) richness, abundance (numbers per haul) and diversity (H') of neuston samples (per station) collected across the Southern Indian Ocean Subtropical Gyre in June/July 2015, by Longitude Class.

Measure	Richness		Abundance		Diversity (H′)	
Time of Day Longitude Class (°E)	Day	Night	Day	Night	Day	Night
65–70	22.00 (1.53)	32.67 (4.26)	652.00 (50.96)	561.33 (170.22)	1.43 (0.03)	1.6 (0.22)
70–75	11.50 (2.09)	27.00 (3.98)	29.50 (5.99)	134.33 (15.46)	2.00 (0.22)	2.52 (0.21)
75–80	10.00 (3.51)	22.67 (1.45)	26.67 (6.94)	141.00 (59.57)	1.99 (0.26)	2.22 (0.08)
80–85	– 	16.00 (2.31)	– 	97.67 (14.24)	– 	2.11 (0.14)
85–90	16.67 (1.80)	21.89 (1.92)	149.83 (62.28)	163.89 (29.79)	1.92 (0.20)	2.11 (0.13)
90–95	12.50 (1.57)	25.33 (2.76)	83.83 (31.16)	326.83 (66.22)	1.65 (0.33)	2.19 (0.04)
95–100	17.00 (1.53)	36.00 (6.66)	121.67 (45.67)	2433.67 (579.29)	1.91 (0.11)	1.34 (0.30)
100–105	19.67 (1.20)	19.67 (3.94)	416.00 (144.34)	351.00 (144.72)	1.73 (0.14)	1.98 (0.09)

maximum was not included in the final model ($R^2 = 0.52$, adjusted $R^2 = 0.36$; Table 6b). The most significant predictors concerned salinity and temperature at 200 m depth.

Interestingly, and perhaps tellingly, in the case of the night-time samples, only the depth of the fluorescence maximum was not significantly related to the structure of assemblages along the transect (Table 7a), and neither was it included in the full, sequential model ($R^2 = 0.65$, adjusted $R^2 = 0.50$; Table 7b). Unlike noted during the daytime,

sea surface parameters had a greater impact on assemblages than those at 200 m.

Information on the abundance and distribution of microplastics collected in the manta trawl samples during the survey have been reported upon previously by Bernal et al. (2020), and it is not our intention to duplicate that work. Rather, we have summarised their results in Supplementary Material D, from which it can be seen that numbers per haul were generally greater in the eastern part of the transect (95–105° E) than elsewhere. Microplastics were least abundant in the centre of the region. There was no relationship between the abundance of microplastics and either the total abundance of facultative neuston ($R = 0.68$, $p = 0.07$) or euneuston ($R = 0.22$, $p = 0.59$).

4. Discussion

During the 12 months prior to the survey, the "centre" of the Southern Indian Ocean Subtropical Gyre lay approximately along latitude 20°S, and extended from ~95° E westwards to the coastline of Madagascar at ~50° E (Fig. 1). At the time of the cruise, its mean position was strongly disrupted by a series of mesoscale eddies (both cyclonic and anticyclonic) ranging in size from 50 to 150 km diameter (Toresen et al., 2015). Two distinct, anticyclonic, warm core eddies, with elevated sea surface heights were detected between 70 and 85° E (Dufois et al., 2017). Conditions in these eddies were distinct from those at the edge, with elevated concentrations of chlorophyll being attributed to deeper convective mixing (Dufois et al., 2017). Assemblages of plankton in the centre of eddies are often distinct from those outside (e.g. Noyon et al., 2019), perhaps because of the horizontal advection of productive waters and deeper vertical mixing in the anticyclonic eddies causing an increase in surface chlorophyll in the anticyclonic eddies in winter in the Southern Indian Ocean Subtropical Gyre (Dufois et al.,
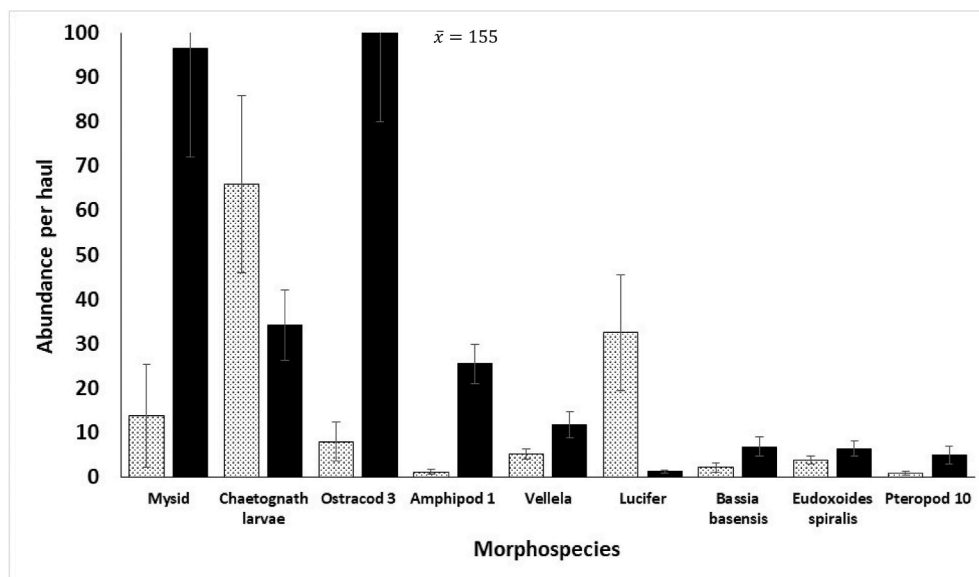

Fig. 4. The average (±se) abundance of the morphospecies responsible for 70% dissimilarity amongst samples collected during the day or night across the Southern Indian Subtropical Gyre during June/July 2015. Data pooled across Longitudinal Class.
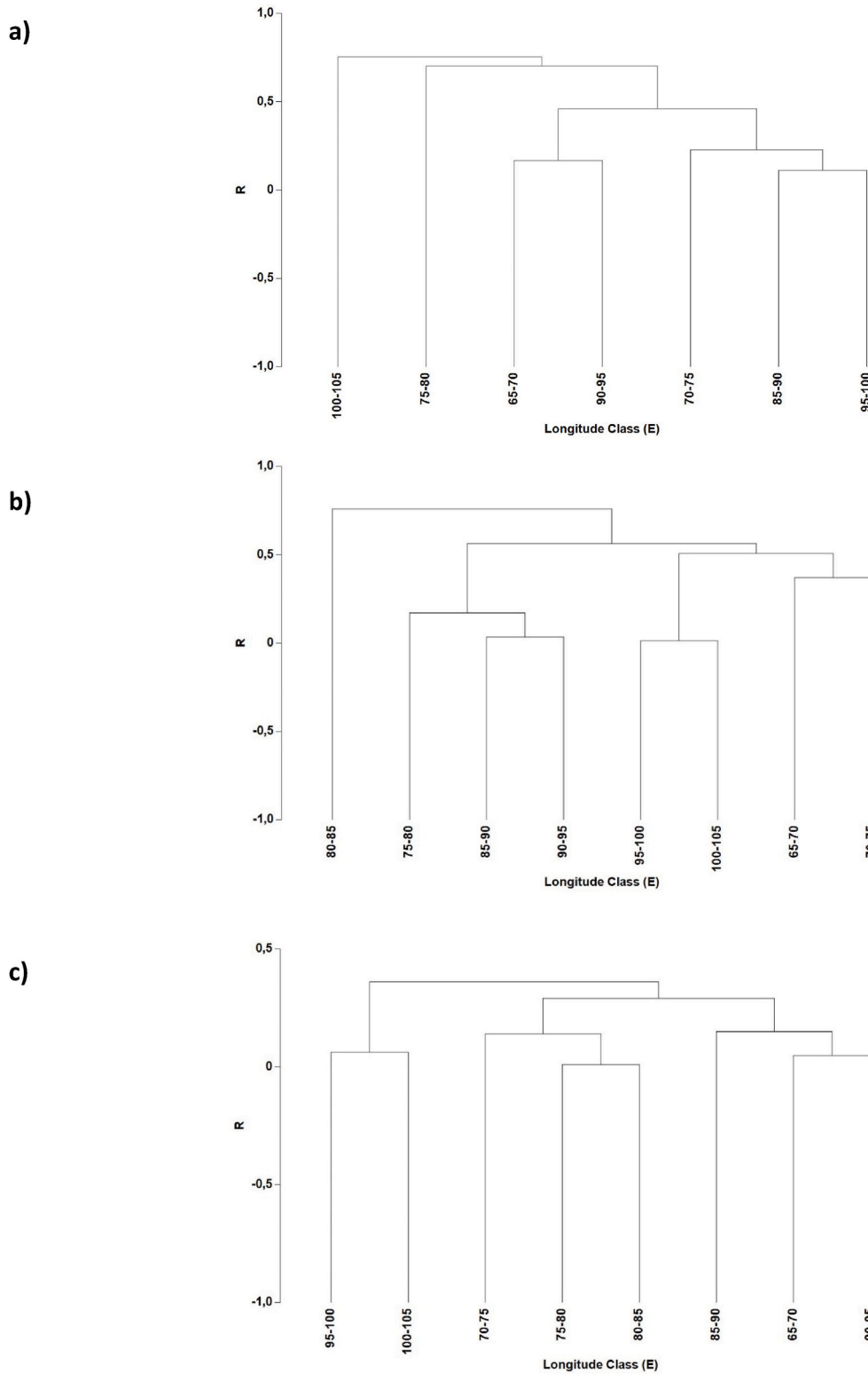
Fig. 5. Pairwise *R* values among neuston assemblages for Longitude Classes across the Southern Indian Subtropical Gyre in June/July 2015, displayed as dendrograms (group-average linkage). Data shown separately by Time of Day: night (a), day (b) all (c).

2017).

4.1. General observations on the neuston

The study conducted here did not take into account copepods, which could represent ~68.5% of total neuston abundance in the region

(Holdway and Maddock, 1983a,b). On balance, the composition of the neuston communities examined is broadly similar to that of previous studies (Zaitsev, 1971; Hempel and Weikert, 1972; Holdway and Maddock, 1983a; Brodeur et al., 1987), being dominated by groups that are known to have a high diversity in the plankton, such as amphipods and pteropods.
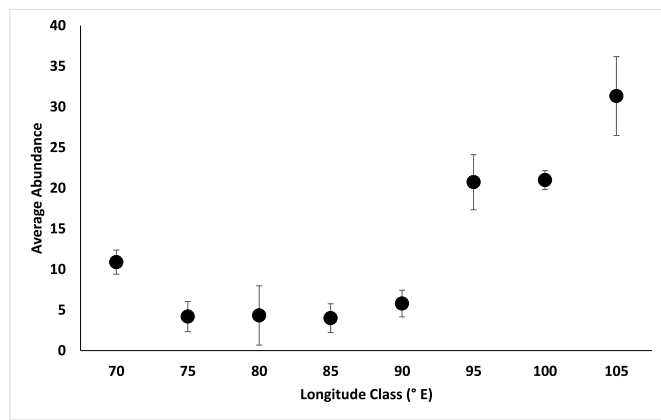
Fig. 6. Changes in the mean (±se) percentage of meroplankton in the neuston assemblages across the Southern Indian Subtropical Gyre during June/ July 2015.

Table 5

The average (±se) abundance and percent contribution to sample identity of the morphospecies responsible for 70% similarity amongst samples in the three distinct areas identified in Fig. 4c, as determined from SIMPER analysis. Data pooled across Time of Day; –, negligible percent contribution.

Cluster	65–70° E, 85–95° E	70–85° E	95–105° E
Abylopsis eschscholtzi	2.36 (0.17) 5.33	2.54 (0.31) 12.25	1.31 (0.35) –
Amphipod sp. 1	1.18 (0.23) 4.43	0.94 (0.4) 5.14	1.47 (0.57) 3.92
Amphipod sp. 9	0.7 (0.14) –	0.26 (0.15) –	0.93 (0.27) 2.95
Bassia bassensis	0.99 (0.31) –	1.32 (0.7) 3.55	0.36 (0.2) –
Chaetognath larvae	1.8 (0.29) 14.66	0.59 (0.48) –	2.66 (0.28) 16.99
Chelophyes contorta	0.99 (0.12) 3.98	1.19 (0.17) 11.24	1.47 (0.19) 9.16
Decapod larva sp. 0	0.83 (0.12) 5.19	0.23 (0.14) –	0.63 (0.28) –
Doliolid spp.	0.3 (0.09) –	0.27 (0.09) –	0.68 (0.2) 1.97
Enneagonum hyalinum	0.58 (0.12) –	0.35 (0.2) 3.53	0.46 (0.12) –
Eudoxoides spiralis	1.26 (0.13) 6.88	1 (0.25) 8.08	0.45 (0.13) –
Fish sp. C	0.47 (0.09) –	0.22 (0.22) –	0.73 (0.29) 2.46
Janthina spp.	0.7 (0.12) 3.54	0.76 (0.35) 3.93	0.3 (0.15) –
Lucifer spp.	0.82 (0.22) 4.11	0.2 (0.2) –	1.15 (0.44) 3.83
Mysid sp A	1.47 (0.28) 6.79	1.18 (0.59) 3.54	2.36 (0.74) 7.97
Ostracod sp. 3	0.86 (0.21) –	0.77 (0.22) –	2.67 (0.94) 7.84
Pteropod sp. 11	0.5 (0.1) –	0.8 (0.3) 3.42	0.78 (0.4) –
Thalia spp.	0.83 (0.08) 4.81	0.64 (0.27) 3.88	0.82 (0.14) 3.58
Vellela vellela	1.54 (0.11) 11.09	1.61 (0.27) 14.8	0.56 (0.32) –
Water strider sp. A	0.2 (0.08) –	0.08 (0.08) –	0.64 (0.25) 1.99
Water strider sp. B	0.48 (0.12) –	0.18 (0.11) –	1.31 (0.3) 6.22
Water strider sp. C	0.17 (0.07) –	0.17 (0.1) –	0.79 (0.19) 2.31

Table 6a

Marginal test results of the DistLM exploring the effect of different environmental variables on the structure of day-time neuston assemblages observed across the Southern Indian Subtropical Gyre in June/July 2015.

Variable	SS (trace)	Pseudo-F	p	Prop.
SST (sea surface temperature)	4183.0	1.9043	0.026	0.06368
Temperature at 200 m	6450.8	3.0492	0.001	0.09821
SSS (sea surface salinity)	4061.8	1.8455	0.034	0.06184
S (salinity) at 200 m	4978.6	2.2962	0.012	0.07579
SSFl (Sea surface fluorescence)	4024.9	1.8277	0.042	0.06127
D Fl max (depth of fluorescence maximum, m)	2619.6	1.1630	0.270	0.03988
Fl at Chl max (fluorescence at chlorophyll maximum)	3524.3	1.5874	0.078	0.05365
Integr Fl (Integrated fluorescence)	4341.4	1.9815	0.021	0.06609
Depth	1798.7	0.7883	0.674	0.02738

The region studied here had previously been investigated by Holdway and Maddock (1983a) in June 1980, as part of a voyage from Fiji to the Bay of Biscay. Thirty-three stations were sampled by Holdway and Maddock (1983a) in "Area 4", which extended from Jakarta to the Seychelles, using a similar net to that employed here, but towed for 30 min (not 15 min) at a speed approximately twice that used here. Unfortunately, however, Holdway and Maddock (1983a) have provided no detailed information on the neuston of individual stations sampled, and they simply pooled data across the area, which restricts any direct comparison with our study. Average neuston abundance in their Area 4 was 1 700±263 organisms haul^{-1} (Holdway and Maddock, 1983a), and if we accept that their nets filtered twice as much water as ours', this equates to an abundance of 850 organisms haul^{-1}. Non-copepod neuston represented ~31.5% of the specimens caught (Holdway and Maddock, 1983a), or ~270 organisms haul^{-1} – a value that is remarkably similar to ours' (overall average of ~310 organisms haul^{-1}).

The diversity of neuston recovered by Holdway and Maddock (1983a) was relatively homogenous with 20±0.8 taxa haul^{-1}, and if one looks at the contribution of dominant taxa (once copepods have been removed) mysids (20.16%), ostracods (10.4%), gastropod larvae (8.8%) and chaetognaths (7.3%) were important (Holdway and Maddock, 1983b). These values are not too dissimilar to those reported here, except gastropod larvae, but see below. This central area of the Indian Ocean was shown by Holdway and Maddock (1983a,b) to have the highest number of euneuston and the least amount of tar/plastic/pumice.

Without going into too much detail, a number of (perhaps random) comments are pertinent here regarding the general composition of the assemblages recovered. Chaetognaths were commoner than might be expected (Hempel and Weikert, 1972; Brodeur et al., 1987), and all specimens were juveniles, and so unidentifiable, which contrasts with the results of other studies. Grant (1991) recorded 17 species of chaetognaths in the hyponeuston of the Mid-Atlantic Bight, noting that they were generally less common there than in sub-surface waters. That said, Grant (1991) did comment upon the fact that species with warm-water and subtropical affinities were more regularly encountered closer to the sea surface than at greater depths. While doliolids were scarce in our study, salps, including morphospecies of *Thalia* (as well as *Traustedtia* and *Salpa*), were frequently encountered across the sampling area. Holdway and Maddock (1983a) also noted their presence in Indian Ocean samples, but few other studies of neuston have remarked on thaliaceans in their collections (but see also Mantha et al., 2019).

Isopods are known to occur in neuston samples, though not frequently and not in large numbers (Holdway and Maddock, 1983a; Brodeur et al., 1987); as here. This possibly reflects the absence of rafting algae and other flotsam (Thiel and Gutow (2004) and references therein), which would also explain the lack of nereid polychaetes (Baker et al., 2018).

Although Rezai et al. (2019) recorded few siphonophores in the neuston of the NE Persian Gulf, (Holdway and Maddock, 1983a) found them to be common across all the transects they investigated: as too they were here. Of the 22 species noted here, eight were recorded in all longitudinal bins and *Abylopsis eschscholtzii* was most abundant followed by *Chelophyes contorta* and *Bassia bassensis* (Supplementary Material B). Similar species (and numbers of species) of siphonophores were recovered amongst assemblages of neuston in the Mozambique Channel (Thibault unpublished data) and very-near the surface in the Colombian Pacific by Uribe-Palomino et al. (2019). The latter authors noted that *Diphyes dispar, Eudoxoides mitra, C. contorta* and *Muggiaea atlantica* were the most common species, respectively. The fact that *M. atlantica* was not recovered here reflects its coastal distribution (e.g. Thibault-Botha et al., 2004), and is no surprise. Interestingly, Uribe-Palomino et al. (2019) recorded few specimens of *B. bassensis*, which together with *A. eschscholtzii* here dominated assemblages around 85° E. This species can be very abundant in subtropical waters (e.g. Pagès et al., 2001) but tends to be uncommon closer to the shelf (e.g. Pagès and Gili, 1992).

Table 6b

Sequential test results of the DistLM exploring the effect of different environmental variables on the structure of day-time neuston assemblages observed across the Southern Indian Subtropical Gyre in June/July 2015. See Table 6a for full labels to variables.

Variable	Adj R^2	SS (trace)	Pseudo-F	p	Prop.	Cumul.	res. df
+Temp @ 200 m	0.065998	6450.8	3.0492	0.001	0.098205	0.09821	28
+S @ 200 m	0.11409	5056.5	2.5199	0.003	0.076979	0.17518	27
+D Ch max (m)	0.16496	5003.0	2.6451	0.004	0.076164	0.25135	26
+SSS	0.21464	4704.7	2.6447	0.001	0.071622	0.32297	25
+Integr Fl (RF)	0.25805	4138.3	2.4625	0.005	0.063001	0.38597	24
+SSFl (RF)	0.29700	3709.9	2.3298	0.011	0.056478	0.44245	23
+SST	0.35630	4547.2	3.1187	0.001	0.069225	0.51167	22

Table 7a

Marginal test results of the DistLM exploring the effect of different environmental variables on the structure of night-time neuston assemblages observed across the Southern Indian Subtropical Gyre in June/July 2015. See Table 6a for full labels to variables.

Variable	SS (trace)	Pseudo-F	p	Prop.
SST	6777,1	4,0267	0,001	0,15471
Temp @ 200 m	5513,5	3,1678	0,003	0,12587
SSS	6457,6	3,804	0,001	0,14742
S @ 200 m	5407,4	3,0983	0,003	0,12345
S Fl (RF)	3928,2	2,1673	0,019	0,089677
D Chl max (m)	2904,6	1,5624	0,095	0,066309
Fl @ Chl max (RF)	6393	3,7595	0,001	0,14595
Integr Fl (RF)	4731,1	2,6638	0,003	0,10801
Depth	5157,6	2,936	0,004	0,11774

Abylopsis eschscholtzii dominated siphonophore assemblages in the tropical Sargasso Sea (Lüskow et al., 2019).

4.2. Diel changes in assemblage structure

As expected, the diversity and abundance of the neuston was higher at night than during the day, following the upward migration of facultative neuston, which move into the surface waters at night in order to feed and escape predators (Williamson et al., 1996). The significant role that the time of day plays in shaping the structure of neuston assemblages has long been recognised (Hempel and Weikert, 1972), and most of the taxa that display this clearly here (e.g. mysids, ostracods, amphipods) are widely known to do so (Angel, 1999; Vinogradov, 1999). Tomopterid and alciopid polychaetes were found exclusively at night, and they have been shown to be very strong migrators in the Sargasso Sea (Eden et al., 2009).

Members of the euneuston generally failed to display pronounced diel changes in abundance (as Weikert, 1970; Grave, 1971; Zaitsev, 1971; Hempel and Weikert, 1972), though morphospecies of *Halobates* and *Velella* were more common by night than by day; hence the significant PERMANOVA result (Table 2c) It could be argued that the diel difference in the abundance of *Halobates* might reflect net avoidance and night blindness, as these animals detect food by sight or via the sensory detection of water ripples created by struggling prey at the ocean surface (Sagaydachnyy, 1975; Cheng, 1985), suggesting a sensory disadvantage at night. But quite why *Velella velella* may be more common at night is somewhat of a mystery: unfortunately the data do not permit a more detailed examination of this fact.

4.3. Meroplankon

The sea-surface represents an important nursery area for many epi- and mesopelagic fish species, and a wide variety of forms can be found there, usually as eggs and larvae (e.g. Doyle, 1992). Although there are relatively few studies of the neustonic ichthyofauna in the open Indian Ocean, Olivar et al. (2015) recorded 14 larval fish taxa along a longitudinal transect at ~25° S, and assemblages were dominated by Myctophidae (as too Egger et al., 2021) and Exocoetidae. Here, only twelve morphospecies were recovered, but as juveniles not larvae: no eggs were collected. Juvenile fish abundances were not particularly high, and most failed to display clear day-night differences in abundance (as Holdway and Maddock (1983a), but unlike Olivar et al. (2015)). Neustonic fish larvae are notoriously patchy in their distribution (Olivar et al., 2015), and this could explain the absence of any spatial pattern to the distribution of assemblages here. That said, diversity and abundance were greater at the eastern part of the transect than in the centre or to the west, probably as a result of contributions from the Indonesian Throughflow (see below).

Other meroplankton was represented by a wide variety of taxa but was dominated, for the most part, by larvae of decapods and stomatopods. Larvae of brachiopods, polychaetes, bryozoans, gastropods, bivalves, and echinoderms were rare or absent altogether, though they were conspicuous in the study of Holdway and Maddock (1983a) from across this same area. Indeed, the latter authors noted that meroplankton represented about 33% of the non-copepod neuston, whereas here they constituted between 3% and 10%, being more abundant at the longitudinal extremes of the transect than at the centre (Fig. 6).

If we accept that waters along the transect have their origin, in part, from the east and from the Indonesian Throughflow (Dufois et al. (2017) and references therein), then perhaps the high numbers of meroplankton found in samples (Fig. 6) collected close to Jakarta and Christmas Island can be explained by their proximity to the Coral or East Indies Triangle (Hoeksema, 2007; Veron et al., 2009). Coral reefs support very rich associated communities, especially of decapods (Klompmaker et al., 2013 and references therein) and stomatopods (Barber et al., 2002), many of which have planktonic larval development. As this advected water moves westward from the coast and into open ocean water (its effects can be felt through to the Agulhas Current in the west; Lee et al.,

Table 7b

Sequential test results of the DistLM exploring the effect of different environmental variables on the structure of night-time neuston assemblages observed across the Southern Indian Subtropical Gyre in June/July 2015. See Table 6a for full labels to variables.

Variable	Adj R^2	SS (trace)	Pseudo-F	p	Prop.	Cumul.	res. df
+SST	0.11629	6777.1	4.0267	0.001	0.15471	0.15471	22
+Fl @ Chl max (RF)	0.20059	5054.3	3.3197	0.001	0.11538	0.27010	21
+Temp @ 200 m	0.24499	3213.8	2.2350	0.015	0.07337	0.34347	20
+S Fl (RF)	0.28413	2854.4	2.0936	0.030	0.06516	0.40863	19
+Integr Fl (RF)	0.37224	4383.9	3.6667	0.001	0.10008	0.50871	18
Depth	0.47572	4546.0	4.5529	0.001	0.10378	0.61249	17
+SSS	0.49722	1653.5	1.7267	0.075	0.03775	0.65024	16

2002), it is likely that the meroplanktonic species drop out of assemblages, as has been noted by Ayata et al. (2011) for polychaetes in the Bay of Biscay, and Meerhof et al. (2018) for decapod larvae around Easter Island. The former of these latter two studies was conducted over a far shorter spatial scale than this one, which serves to emphasise the effect and as a consequence it is perhaps no surprise that the number of such benthic meroplankton are low between 75 and 85°E.

Moving further westward still, the numbers of larval zooanthids, decapods and stomatopods once again begin to increase, which could reflect the southward advection of waters from the Mascarene Plateau, because the diversity of both taxa is known to be relatively high off the east coast of Africa (Reaka et al., 2008; Head et al., 2018).

4.4. Longitudinal patterns displayed by neuston

The use of morphospecies complicates clear interpretation of the longitudinal patterns because, as noted earlier, a single morphospecies may comprise more than one sibling species, whilst different developmental stages of the same species, may be regarded here as representing separate morphospecies. The latter is especially likely to occur in the case of larval decapods, polychaetes and even fish larvae, whose anatomy and outward appearance may change quite markedly during development (Williamson, 2013). The other taxon that is particularly problematic in this regard is Pteropoda, species of which can usually be identified by the shape of their calcareous shell (e.g. van der Spoel and Dadon, 1999). Unfortunately, following prolonged exposure to preservatives, the shells of pteropods had all but dissolved, and animals were separated on the basis of the shape of the remaining body mass and wing-like feet; when the latter had not been retracted. Regardless, every effort was made to be consistent in specimen categorisation to morphospecies and so it is hoped that errors were consistent across the samples (Supplementary Material A).

If we accept the above, and are conservative in our interpretation of the results, then the results suggest the following. Firstly, the easternmost assemblages (Longitude Classes 100 and 105) are distinct (Fig. 5c); secondly, assemblages between 70 and 85° E (corresponding to Longitude Classes 75, 80 and 85) are distinct (Fig. 5c) and that there is an approximate symmetry of the remaining samples around that (Fig. 5c). The fact that both facultative neuston and euneuston demonstrate at least elements of this pattern when examined separately gives us confidence in this interpretation (but see below).

The high diversity and distinct nature of assemblages between 95 and 105° E no doubt reflects the impact of water emerging from the Java and Banda Seas in the Indonesian Throughflow. As noted previously, the East Indies Triangle is a global biodiversity hotspot (e.g. Roberts et al., 2002) for many benthic or reef associated taxa and is likely to have high levels of plankton diversity too (e.g. Yasuhara et al., 2012). This area was characterised by relatively high temperatures (>25 °C) and low salinities (<34.75) at the surface and neuston assemblages delimited by water-striders, doliolids and high numbers of chaetognath larvae, *Lucifer,* and mysids: zoanthid larvae were also common. Morphospecies of *Thalia* were also common.

It is likely that the neuston were being impacted by the eddies observed to be present between 70 and 85° E during the cruise (see above), because assemblages in this region were generally less abundant, species-rich and diverse than those to either the east or the west. The near absence of meroplankton in these samples is perhaps no surprise, given that the majority of taxa would likely be of benthic forms (e.g. Brandão et al., 2020; Descôteaux et al., 2021) and the great distance of this region from the coast, as has been argued above. But we need to remember too that the plankton sampled here is neuston – it is not a representative of the wider zooplankton in this region. As a consequence, we should not perhaps expect neuston to (e.g.) increase in abundance in response to the elevated Chl *a* associated with the anticyclonic gyres noted (Dufois et al., 2017).

That said, the sequential tests of the DistLM indicate some aspects of the chlorophyll environment (sea surface fluorescence, integrated fluorescence and depth of the fluorescence maximum) were all correlated with neuston assemblage structure during the day (Table 6b). As too were features of the water column at 200 m (Table 6b). This contrasts with the situation at night, when some surface features were more important (including SST), together with some similar, but some different, aspects of the fluorescence environment (sea surface fluorescence, integrated fluorescence, the value of fluorescence at the fluorescence maximum but not the depth of the fluorescence maximum) (Table 7b). Although the relative importance of deep (day) or shallow (night) features of the environment on neuston assemblages is not surprising, it is also telling – implying that during the day at least, migrating facultative taxa are responding to conditions at the bottom of the epipelagos, whilst during the night, surface features are more important in this regard. Diel vertical migration is widely regarded as flexible, and it is strongly influenced by the external environment (Bandara et al., 2021).

The euneuston is dominated by carnivores: *Physalia* (Bieri, 1970; Holdway and Maddock, 1983a), *Velella* (Purcell et al., 2015; Betti et al., 2019; Helm, 2021b), *Porpita* (Sahu et al., 2020), *Janthina* (Churchill et al., 2011; Helm, 2021b), *Glaucus* (Thompson and Bennett, 1970; Sahu et al., 2020; Helm, 2021b) and *Halobates* (Cheng, 1985) all eat "meat". And carnivores dominated the abundance of the non-copepod neuston westward of 95°E. Yet euneuston only represented 11% of the fauna between 70 and 85°E (Table 1), less than 6% of assemblages in most other samples there and only 2% of that eastward of 95°E. The carnivorous nature of the neuston is largely down to its facultative members, because chaetognaths (Albuquerque et al., 2021), siphonophores (Mackie et al., 1988) and most hyperiid amphipods (Shulenberger, 1977) also eat "meat". Although we should be cautious in our interpretation of these data because information about copepods is missing, neustonic copepods show a greater tendency towards carnivory/omnivory than herbivory (e.g. Kerambrun and Champalbert, 1995). And this can be seen very clearly in the overlapping isoplots of Albuquerque et al. (2021). In other words, not only do the organisms that occupy the sea-surface interphase look different from those occurring at depths greater than 30 cm (Helm, 2021a), but the assemblages of which they are part likely function in slightly different ways – at least towards the centre of subtropical ocean gyres.

Although we have stressed the similarities in the patterns between facultative neuston and euneuston here (Fig. 5, Supplementary Material C), there are differences in the spatial distribution of each. This is hardly surprising given that euneuston are bound to the sea-surface interphase, whereas facultative neuston are not. Thus, euneuston may be more susceptible to the effects of trade winds, while facultative neuston are more likely to be influenced by the properties and origins of the underlying water masses. Unfortunately, however, given the relatively few number of stations sampled for nekton, it is not possible to comment further without speculation.

4.5. Neuston and microplastics

Bernal et al. (2020) have previously discussed the microplastic data reported on here, albeit primarily in the context of ingestion by mesopelagic fishes, and there is little we can add. They too noted that microplastic abundance was greater at the edges of the gyre than at the centre, and they remarked on the fact that the ingestion of microplastics by mesopelagic fishes was much less marked than in other subtropical gyre systems. These authors stressed however, that information on the abundance and distribution of microplastics in the central Indian Ocean is effectively non-existent, which makes more detailed comparisons difficult, and they recommended that more work be undertaken in this regard: a comment we echo. Holdway and Maddock (1983b) recorded very few tar/plastic/pumice particles amongst neuston samples collected in the Indian Ocean, certainly by comparison with the other areas sampled, though to be fair the majority of the other areas were

closer to the coast. Unfortunately, owing to the fact that Holdway and Maddock (1983b) measured this debris in units of mg.m^{-2}, we are not in a position to compare our data. Assuming an average towing speed of 2.5 knots and an average microplastic concentration of ~31.1 particles per manta haul (SD = 43.6), the density of microplastics across the survey transect is ~86 714 particles.km^{-2}. This value is greater than that noted by Egger et al. (2021) from neuston samples collected outside the North Pacific Gyre (6 150 particles.km^{-2}) but significantly less than these authors noted at either the edge (245 833 particles.km^{-2}) or at the centre (214 625 particles.km^{-2}) of that gyre. Interestingly, the average number of microplastic particles per non-copepod neuston member observed here is lower (0.10) than that noted by Egger et al. (2021) outside the North Pacific Gyre (0.13), and much lower than seen at either the edge (14.25) or centre (19.96) of that system.

Using the positions of ocean surface drifters, van der Mheen et al. (2019) derived transport matrices to simulate the accumulation of buoyant debris in the southern Indian Ocean. These authors noted that the behaviour of surface particles in the Indian Ocean is distinct from that seen in other ocean basins. Indeed, they observed a greater accumulation of "microplastics" to the western side of the gyre than in the centre, which they attributed to "… the strong easterly trade winds in the Southern Indian Ocean as well as the unique geography at the western boundary of the Southern Indian Ocean Gyre" (van der Mheen et al., 2019, pp2588). Regardless of the physics driving the distribution and accumulation of microplastics in the central Indian Ocean, which is still not well documented, there was clearly little link between them and the neuston – either facultative or euneuston. Which is perhaps somewhat perplexing, given that most euneuston (excluding *Janthina* and *Glaucus*) project above the sea-surface interphase and are more likely to be influenced by the trade winds. Egger et al. (2021) also failed to observe a positive relationship between the abundance of different neustonic organisms and microplastics in the North Pacific Gyre. These authors noted that, unlike the situation here, the abundance of marine debris was greatest in the centre of the gyre which, like here, also supported lowest densities of neuston (copepods excepted).

5. Conclusions

Overall, the results of the study were in accordance with much of the previous literature in terms of the general taxa present, though they differed in some respects. The preponderance of ostracods and juvenile chaetognaths in samples was unusual, while the lack of flotsam meant that many of those organisms that inhabit such structures were missing. The fact that assemblages were generally more diverse towards the margins of the transect is no surprise, given that holoplankton was being supplemented with meroplankton – especially in the east with water from the Indonesian Throughflow: this is as originally hypothesised. Communities were strongly influenced by the time of day, reflecting the diel vertical migration of facultative members, whose abundances and diversity were all greater at night: which again comes as no surprise.

There was a strong agreement between the structure of assemblages and the structure of the physical environment, and assemblages in the core of the anticyclonic eddies were distinctly different from those outside, as initially hypothesised. In part this may reflect the drop-out of meroplanktonic forms, but there is a suggestion in the data that the chlorophyll environment may have some role to play in this. More work that couples the physical environment with the neuston is clearly needed, though this study emphasises the value of simultaneously collected data sets in this regard.

This study used morphospecies as identification units, rather than recognised species (with the exception of siphonophores), and we believe this approach holds much promise for future work. It does have its drawbacks as articulated previously, but it does allow, by comparison with (e.g.) ZooScan, a greater resolution in taxonomic identification (Gorsky et al., 2010), without the need for full-blown training in the taxonomy of individual taxa. It is unlikely to be as thorough in its

resolution of species units as e-DNA (Garcia-Vazquez et al., 2021) or molecular approaches to identification (Bucklin et al., 2021), but in an African context where the cost of such technologies is so high (let alone the specialist laboratories needed to undertake the work), it does have its advantages (see also Machida et al., 2021).

Declaration of competing interest

The authors declare that they have no known competing financial interests or personal relationships that could have appeared to influence the work reported in this paper.

Data availability

Data will be made available on request.

Appendix A. Supplementary data

Supplementary data to this article can be found online at https://doi.org/10.1016/j.dsr2.2022.105249.

References

Albuquerque, R., Bode, A., González-Gordillo, J.I., Duarte, C.M., Queiroga, H., 2021. Trophic structure of neuston across tropical and subtropical oceanic provinces assessed with stable isotopes. Front. Mar. Sci. 7, 1205.

Anderson, M.J., Gorley, R.N., Clarke, K.R., 2008. PERMANOVA+ for PRIMER: Guide to Software Statistical Methods. PRIMER-E, Plymouth.

Andersen, N.A., Cheng, I., 2004. The marine insect *Halobates* (Heteroptera: Gerridae): biology, adaptations, distribution, and phylogeny. Oceanogr. Mar. Biol. Annu. Rev. 42, 119–180.

Angel, M.V., 1999. Ostracoda. In: Boltovskoy, D. (Ed.), South Atlantic Zooplankton. Backhuys Publishers, Leiden, pp. 815–868.

Ayata, S.D., Stolba, R., Comtet, T., Thiébaut, É., 2011. Meroplankton distribution and its relationship to coastal mesoscale hydrological structure in the northern Bay of Biscay (NE Atlantic). J. Plankton Res. 33, 1193–1211.

Baker, P., Minzlaff, U., Schoenle, A., Schwabe, E., Hohlfeld, M., Jeuck, A., Brenke, N., Prausse, D., Rothenbeck, M., Brix, S., Frutos, I., 2018. Potential contribution of surface-dwelling *Sargassum* algae to deep-sea ecosystems in the southern North Atlantic. Deep Sea Res. II 148, 21–34.

Bandara, K., Varpe, Ø., Wijewardene, L., Tverberg, V., Eiane, K., 2021. Two hundred years of zooplankton vertical migration research. Biol. Rev. 96, 1547–1589.

Barber, P.H., Moosa, M.K., Palumbi, S.R., 2002. Rapid recovery of genetic diversity of Stomatopod populations on Krakatau: temporal and spatial scales of marine larval dispersal. Proc. R. Soc. Ser. B 269, 1591–1597.

Bernal, A., Toresen, R., Riera, R., 2020. Mesopelagic fish composition and diets of three myctophid species with potential incidence of microplastics, across the southern tropical gyre. Deep Sea Res. II. 179, 104706.

Betti, F., Bo, M., Enrichetti, F., Manuele, M., Cattaneo-Vietti, R., Bavestrello, G., 2019. Massive strandings of *Velella velella* (Hydrozoa: Anthoathecata: Porpitidae) in the Ligurian sea (North-western Mediterranean sea). The European Zool. J. 86, 343–353.

Bieri, R., 1970. The food of *Porpita* and niche separation in three neuston coelenterates. Publ. Seto Mar. Biol. Lab. 17, 305–307.

Brach, L., Deixonne, P., Bernard, M.F., Durand, E., Desjean, M.-C., Perez, E., van Sebille, E., ter Halle, A., 2018. Anticyclonic eddies increase accumulation of microplastic in the North Atlantic subtropical gyre. Mar. Pollut. Bull. 126, 191–196.

Brandão, M.C., Garcia, C.A.E., Freire, F., 2020. Meroplankton community structure across oceanographic fronts along the South Brazil Shelf. J. Mar. Syst. 208, 103361.

Brix, H., Gruber, N., Keeling, C.D., 2004. Interannual variability of the upper ocean carbon cycle at station ALOHA near Hawaii. Global Biogeochem. Cycles 18, GB4019.

Brodeur, R.D., Pearcy, W.G., Mundy, B.C., Wisseman, R.W., 1987. The Neustonic Fauna in Coastal Waters of the Northeast Pacific: Abundance, Distribution, and Utilization by Juvenile Salmonids. Oregon State University Sea Grant Program Report, pp. 1–61.

Bucklin, A., Peijnenburg, K.T.C.A., Kosobokova, K., Machida, R.J., 2021. New insights into biodiversity, biogeography, ecology, and evolution of marine zooplankton based on molecular approaches. ICES J. Mar. Sci. 78, 3281–3287.

Cheng, L., 1985. Biology of *Halobates* (Heteroptera: Gerridae). Annu. Rev. Entomol. 30, 111–135.

Churchill, C.K., Strong, E.E., Ó Foighil, D., 2011. Hitchhiking juveniles in the rare neustonic gastropod *Recluzia* cf. Jehennei (Janthinidae). J. Molluscan Stud. 77, 441–444.

Clarke, K.R., Gorley, R.N., 2015. PRIMER V7 User Manual/Tutorial. PRIMER-E, Plymouth.

Collard, F., Collignon, A., Hecq, J.H., Michel, L.N., Goffart, A., 2015. Biodiversity and seasonal variations of zooneuston in the northwestern Mediterranean sea. Belg. J. Zool. 145, 40–48.

Darwin, C., 1859. On the Origin of the Species by Means of Natural Selection, or the Preservation of Favoured Races in the Struggle for Life. John Murray, London.

de Puelles, M.L., Gazá, M., Cabanellas-Reboredo, M., Santandreu, M.D., Irigoien, X., González-Gordillo, J.I., Duarte, C.M., Hernández-León, S., 2019. Zooplankton abundance and diversity in the tropical and subtropical ocean. Diversity 11, 203.

Descôteaux, R., Ershova, E., Wangensteen, O.S., Præbel, K., Renaud, P.E., Cottier, F., Bluhm, B.A., 2021. Meroplankton diversity, seasonality and life-history traits across the barents sea polar front revealed by high-throughput DNA barcoding. Front. Mar. Sci. 8, 677732.

de Wolf, P., 1989. The price of patchiness. Helgol. Meeresunters. 43, 263–273.

Doyle, M.J., 1992. Neustonic ichthyoplankton in the northern region of the California Current ecosystem. Calif. Coop. Ocean. Fish. Investig. Rep. 33, 141–161.

Dufois, F., Hardman-Mountford, N.J., Greenwood, J., Richardson, A.J., Feng, M., Matear, R.J., 2016. Anticyclonic eddies are more productive than cyclonic eddies in subtropical gyres because of winter mixing. Sci. Adv. 2, e1600282.

Dufois, F., Hardman-Mountford, N.J., Fernandes, M., Wojtasiewicz, B., Shenoy, D., Slawinski, D., Gauns, M., Greenwood, J., Toresen, R., 2017. Observational insights into chlorophyll distributions of subtropical South Indian Ocean eddies. Geophys. Res. Lett. 44, 3255–3264.

Eden, B.R., Steinberg, D.K., Goldthwait, S.A., McGillicuddy, D.J., 2009. Zooplankton community structure in a cyclonic and mode-water eddy in the Sargasso Sea. Deep Sea Res. I. 56, 1757–1776.

Egger, M., Quiros, L., Leone, G., Ferrari, F., Boerger, C.M., Tishler, M., 2021. Relative abundance of floating plastic debris and neuston in the eastern North Pacific Ocean. Front. Mar. Sci. 8, 566.

Eriksen, M., Maximenko, N., Thiel, M., Cummins, A., Lattin, G., Wilson, S., Hafner, J., Zellers, A., Rifman, S., 2013. Plastic pollution in the South Pacific subtropical gyre. Mar. Pollut. Bull. 68, 71–76.

Feng, M., Zhang, N., Liu, Q., Wijffels, S., 2018. The Indonesian throughflow, its variability and centennial change. Geosci. Lett. 5, 3.

Follows, M.J., Ito, T., Marotzke, J., 2002. The wind-driven, subtropical gyres and the solubility pump of CO_2. Global Biogeochem. Cycles 16, 60–61, 60-9.

Garcia-Vazquez, E., Georges, O., Fernandez, J., Ardura, A., 2021. DNA metabarcoding of small plankton samples to detect fish larvae and their preys from Atlantic and Pacific waters. Sci. Rep. 11, 7224.

Goldstein, M.C., Rosenberg, M., Cheng, L., 2012. Increased oceanic microplastic debris enhances oviposition in an endemic pelagic insect. Biol. Lett. 8, 817–820.

González, C.E., Escribano, R., Bode, A., Schneider, W., 2019. Zooplankton taxonomic and trophic community structure across biogeochemical regions in the Eastern South Pacific. Front. Mar. Sci. 5, 498.

Gorsky, G., Ohman, M.D., Picheral, M., Gasparini, S., Stemmann, L., Romagnan, J.-B., Cawood, A., Pesant, S., García-Comas, C., Prejger, F., 2010. Digital zooplankton image analysis using the ZooScan integrated system. J. Plankton Res. 32, 285–303.

Grant, G.C., 1991. Chaetognatha from the central and southern Middle Atlantic Bight - species composition, temperature-salinity relationships, and interspecific associations. Fish. Bull. 89, 33–40.

Grave, H., 1971. Kurzzeitige Sehwankungen im Neuston der Norwegischen See. Diplom-Arbeit, Universitgt Kiel.

Head, C.E., Bonsall, M.B., Jenkins, T.L., Koldewey, H., Pratchett, M.S., Taylor, M.L., Rogers, A.D., 2018. Exceptional biodiversity of the cryptofaunal decapods in the Chagos Archipelago, central Indian Ocean. Mar. Pollut. Bull. 135, 636–647.

Helm, R.R., 2021a. The mysterious ecosystem at the ocean's surface. PLoS Biol. 19, e3001046.

Helm, R.R., 2021b. Natural history of neustonic animals in the Sargasso Sea: reproduction, predation, and behavior of Glaucus atlanticus, Velella velella, and Janthina spp. Mar. Biodivers. 51, 99.

Hempel, G., Weikert, H., 1972. The neuston of the subtropical and boreal North-eastern Atlantic Ocean A review. Mar. Biol. 13, 70–88.

Herring, P.J., 1967. Blue pigment of a surface-living oceanic copepod. Nature 205, 103–104.

Hoeksema, B.W., 2007. Delineation of the Indo-Malayan centre of maximum marine biodiversity: the Coral Triangle. In: Renema, W. (Ed.), Biogeography, Time, and Place: Distributions, Barriers, and Islands. Springer, Dordrecht, pp. 117–178.

Holdway, P., Maddock, L., 1983a. A comparative survey of neuston: geographical and temporal distribution patterns. Mar. Biol. 76, 263–270.

Holdway, P., Maddock, L., 1983b. Neustonic distributions. Mar. Biol. 77, 207–214.

Hood, R.R., Urban, E.R., McPhaden, M.J., Su, D., Raes, E., 2016. The 2nd international Indian Ocean Expedition (IIOE-2): Motivating new exploration in a Poorly understood basin. Limnol. Oceanogr. Bull. 25, 117–124.

Ianora, A., Miraito, A., Vanucci, S., 1992. The surface attachment structure: a unique type of integumental formation in neustonic copepods. Mar. Biol. 113, 401–407.

Jeong, H.G., Suh, H.-L., Lee, W., Soh, H.Y., 2014. Seasonal variation of the neustonic zooplankton community in southern waters of Korea. Ocean Sci. J. 49, 167–181.

Kerambrun, P., Champalbert, G., 1995. Diel variations of gut fluorescence in the pontellid copepod *Anomalocera patersoni*. Comp. Biochem. Physiol. A 111, 237–239.

Klompmaker, A.A., Ortiz, J.D., Wells, N.A., 2013. How to explain a decapod crustacean diversity hotspot in a mid-Cretaceous coral reef. Palaeogeogr. Palaeoclimatol. Palaeoecol. 374, 256–273.

Krebs, C.J., 1999. Ecological Methodology. Benjamin/Cummings, Menlo Park.

Kuyper, D., Thibault, D., Gibbons, M.J., 2020. Latitudinal changes in siphonophore assemblages across the Atlantic sector of the Southern Ocean. Afr. J. Mar. Sci. 42, 209–219.

Lebreton, L., Slat, B., Ferrari, F., Sainte-Rose, B., Aitken, J., Marthouse, R., Hajbane, S., Cunsolo, S., Schwarz, A., Levivier, A., Noble, K., Debeljak, P., Maral, H., Schoeneich-Argent, R., Brambini, R., Reisser, J., 2018. Evidence that the great Pacific garbage Patch is rapidly accumulating plastic. Sci. Rep. 8, 4666.

Lee, T., Fukumori, I., Menemenlis, D., Xing, Z., Fu, L.-L., 2002. Effects of the Indonesian throughflow on the Pacific and Indian Oceans. J. Phys. Oceanogr. 32, 1404–1429.

Lüskow, F., Neitzel, P., Miller, M.J., Marohn, L., Wysujack, K., Freese, M., Pohlmann, J. D., Hanel, R., 2019. Distribution and abundance of net-captured calycophoran siphonophores and other gelatinous zooplankton in the Sargasso Sea European eel spawning area. Mar. Biodivers. 49, 2333–2349.

Machida, R.J., Kurihara, H., Nakajima, R., Sakamaki, T., Lin, Y.-Y., Furusawa, K., 2021. Comparative analysis of zooplankton diversities and compositions estimated from complement DNA and genomic DNA amplicons, metatranscriptomics, and morphological identifications. ICES J. Mar. Sci. 78, 3428–3443.

Mackie, G.O., Pugh, P.R., Purcell, J.E., 1988. Siphonophore biology. Adv. Mar. Biol. 24, 97–262.

Mann, K.H., Lazier, J.R.N., 2006. Dynamics of Marine Ecosystems. Blackwell Publishing, Malden.

Mantha, G., Al-Sofyani, A.A., Ali, M., , A.A., Crosby, M.P., 2019. Zooneuston and zooplankton abundance and diversity in relation to spatial and nycthemeral variations in the Gulf of Aqaba and northern Red Sea. Acta Oceanol. Sin. 38, 59–72.

McGillicuddy, D.J., Robinson, A.R., 1997. Eddy induced nutrient supply and new production in the Sargasso Sea. Deep-Sea Res. I 44, 1427–1449.

McGowan, J.A., Walker, P.W., 1985. Dominance and diversity Maintenance in an Oceanic ecosystem: ecol. Monograph 55, 103–118.

Meerhoff, E., Ramos, M., Yannicelli, B., Bravo, L., Zambra, D., Varela, C., 2018. Meroplankton distribution in South Pacific islands, implications for larval connectivity. J. Plankton Res. 40, 77–90.

Mojib, N., Thimma, M., Kumaran, M., Sougrat, R., Irigoien, X., 2017. Comparative metatranscriptomics reveals decline of a neustonicplanktonic population. Limnol. Oceanogr. 62, 299–310.

Morin, P.J., 2011. Community Ecology. John Wiley and Sons, Chichester.

Naumann, E., 1917. Beiträge zur kenntnis des teichnanoplanktons. II. Über das neuston des süßwasser. Biol. Zentralblatt 37, 98–106.

Noyon, M., Morris, T., Walker, D., Huggett, A., 2019. Plankton distribution within a young cyclonic eddy off south-western Madagascar. Deep Sea Res. II 166, 141–150.

Olivar, M.P., González-Gordillo, J.I., Salat, J., Chust, G., Cózar, A., Hernández-León, S., de Puelles, M.L., Irigoien, X., 2015. The contribution of migratory mesopelagic fishes to neuston fish assemblages across the Atlantic, Indian and Pacific Oceans. Mar. Freshw. Res. 67, 1114–1127.

Pagès, F., Gili, J.-M., 1992. Siphonophores (Cnidaria: Hydrozoa) of the benguela current (southeastern atlantic). Sci. Mar. 56 (S1), 65–112.

Pagès, F., González, H.E., Ramón, M., Sobarzo, M., Gili, J.-M., 2001. Gelatinous zooplankton assemblages associated with water masses in the Humboldt Current System, and potential predatory impact by *Bassia bassensis* (Siphonophora: Calycophorae). Mar. Ecol. Prog. Ser. 210, 13–24.

Pakhomov, E.A., Perissinotto, R., McQuaid, C.D., Froneman, P.W., 2000. Zooplankton structure and grazing in the Atlantic sector of the Southern Ocean in late austral summer 1993. Part 1. Ecological zonation. Deep-Sea Res. I. 47, 1663–1686.

Piontkovski, S.A., Landry, M.R., Finenko, Z.Z., Kovalev, A.V., Williams, R., Gallienne, C. P., Mishonov, A.V., Skryabin, V.A., Tokarev, Y.N., Nikolsky, V.N., 2003. Plankton communities of the South Atlantic anticyclonic gyre. Oceanol. Acta 3, 255–268.

Pos, E., Guevara Andino, J.E., Sabatier, D., Molino, J.F., Pitman, N., Mogollón, H., Neill, D., Cerón, C., Rivas, G., Di Fiore, A., Thomas, R., Tirado, M., Young, K.R., Wang, O., Sierra, R., García-Villacorta, R., Zagt, R., Palacios, W., Aulestia, M., ter Steege, H., 2014. Are all species necessary to reveal ecologically important patterns? Ecol. Evol. 4, 4626–4636.

Purcell, J.E., Milisenda, G., Rizzo, A., Carrion, S.A., Zampardi, S., Airoldi, S., Zagami, G., Guglielmo, L., Boero, F., Doyle, T.K., Piraino, S., 2015. Digestion and predation rates of zooplankton by the pleustonic hydrozoan *Velella velella* and widespread blooms in 2013 and 2014. J. Plankton Res. 37, 1056–1067.

Rahlff, J., Ribas-Ribas, M., Brown, S.M., Mustaffa, N.I.H., Renz, J., Peck, M.A., Bird, K., Cunliffe, M., Melkonian, K., Zappa, C.J., 2018. Blue pigmentation of neustonic copepods benefits exploitation of a prey-rich niche at the air-sea boundary. Sci. Rep. 8, 11510.

Reaka, M.L., Rodgers, P.J., Kudla, A.U., 2008. Speciation extinction dynamics and the topography of diversity on Indo-West Pacific coral reefs. In: Riegl, B.B., Dodge, R.E., Hubbard, D.K. (Eds.), Proceedings of the 11th International Coral Reef Symposium. National Coral Reef Institute, Dania Beach, pp. 1377–1381.

Rezai, H., Kabiri, K., Arbi, I., Amini, N., 2019. Neustonic zooplankton in the northeastern Persian Gulf. Reg. Stud. Mar. Sci. 26, 100473.

Roberts, C.M., McClean, C.J., Veron, J.E., Hawkins, J.P., Allen, G.R., McAllister, D.E., Mittermeier, C.G., Schueler, F.W., Spalding, M., Wells, F., Vynne, C., 2002. Marine biodiversity hotspots and conservation priorities for tropical reefs. Science 295, 1280–1284.

Sagaydachnyy, A.Y., 1975. Distribution and some biological characteristics of *Halobates* (Hemiptera. Gerridae) in the Indian Ocean. Oceanology 15, 211–214.

Sahu, B.K., Baliarsingh, S.K., Samanta, A., Srichandan, S., Singh, S., 2020. Mass beach stranding of blue button jellies (*Porpita porpita*, Linnaeus, 1758) along Odisha coast during summer season. Ind. J. Geo-Mar. Sci. 49, 1093–1096.

Shulenberger, E., 1977. Hyperiid amphipods from the zooplankton community of the North Pacific central gyre. Mar. Biol. 1977, 375–385.

Stramma, L., Lutjeharms, J.R.E., 1997. The flow field of the subtropical gyre of the South Indian Ocean. J. Geophys. Res. 102, 5513–5530.

Thibault-Botha, D., Lutjeharms, J.R., Gibbons, M.J., 2004. Siphonophore assemblages along the east coast of South Africa; mesoscale distribution and temporal variations. J. Plankton Res. 26, 1115–1128.

Thiel, M., Gutow, L., 2004. The ecology of rafting in the marine environment. I. The floating substrata. Oceanogr. Mar. Biol. Annu. Rev. 42, 181–264.

Thompson, T.E., Bennett, I., 1970. Observations on Australian Glaucidae (Mollusca: Opisthobranchia). Zool. J. Linn. Soc. 49, 187–197.

Toresen, R., Fulanda, B.M., Dufois, F., Puckridge, M., Fernandes, M., Bernal, A.B., Bagøien, E., Cedras, R., Semili, P., Lutfiyati, I., Utama, A.A., , Nasirin, Theresine, P., Nomenisoa, A.L.D., Torkildson, K.N., Beck, A., 2015. Cruise Reports 'Dr Fridtjof Nansen', Survey of the Southern Indian Ocean Jakarta to Port Louis, IOS Leg 1, p. 26. June -16 July 2015. 2015. Norad, Bergen.

Uribe-Palomino, J., López, R., Gibbons, M.J., Gusmão, F., Richardson, A.J., 2019. Siphonophores from surface waters of the Colombian Pacific Ocean. J. Mar. Biol. Assoc. U. K. 99, 67–80.

van der Mheen, M., Pattiaratchi, C., van Sebille, E., 2019. Role of Indian Ocean dynamics on accumulation of buoyant debris. J. Geophys. Res.: Oceans 124, 2571–2590.

van der Spoel, S., Dadon, J.R., 1999. Pteropoda. In: Boltovskoy, D. (Ed.), South Atlantic Zooplankton. Backhhuys Publishers, Leiden, pp. 649–706.

Veron, J.E., Devantier, L.M., Turak, E., Green, A.L., Kininmonth, S., Stafford-Smith, M., Peterson, N., 2009. Delineating the coral triangle. Galaxea. J. Coral Reef Stud. 11, 91–100.

Vinogradov, G., 1999. Amphipoda. In: Boltovskoy, D. (Ed.), South Atlantic Zooplankton. Backhuys Publishers, Leiden, pp. 1141–1240.

Weikert, H., 1970. Verteilung und Tagesperiodik des Evertebratenneuston im subtropischen Nordostatlantik. Christian-Albrechts-Universität Kiel. 1970, Kiel, p. 170. Doctoral dissertation.

Whitney, J.L., Gove, J.M., McManus, M.A., Smith, K.A., Lecky, J., Neubauer, P., Phipps, J.E., Contreras, E.A., Kobayashi, D.R., Asner, G.P., 2021. Surface slicks are pelagic nurseries for diverse ocean fauna. Sci. Rep. 11, 3197.

Williams, R., Follows, M., 2011. Cycling and transport of nutrients and carbon. In: Ocean Dynamics and the Carbon Cycle: Principles and Mechanisms. Cambridge University Press, Cambridge, pp. 260–289.

Williamson, C.E., Sanders, R.W., Moeller, R.E., Stutzman, P.L., 1996. Utilization of subsurface food resources for zooplankton reproduction: implications for diel vertical migration theory. Limnol. Oceanogr. 41, 224–233.

Williamson, D., 2013. Larvae and Evolution: toward a New Zoology. Springer, Dordrecht.

Yasuhara, M., Hunt, G., Dowsett, H.J., Robinson, M.M., Stoll, D.K., 2012. Latitudinal species diversity gradient of marine zooplankton for the last three million years. Ecol. Lett. 15, 1174–1179.

Zaitsev, Y.P., 1971. Marine Neustonology. Academy of Sciences of the Ukrainian SSR (Kiev. [In Russian]).